*Article*

# Superhydrophobic SiO$_2$/Trimethylchlorosilane Coating for Self-Cleaning Application of Construction Materials

Aliya Kurbanova [1] , Nurbala Myrzakhmetova [2] , Nazgul Akimbayeva [2], Kazhmukhan Kishibayev [2],
Marzhan Nurbekova [2], Yernar Kanagat [3], Arailym Tursynova [3], Tomiris Zhunussova [1] , Aidar Seralin [1] ,
Rabiga Kudaibergenova [4] , Zhexenbek Toktarbay [1],* and Olzat Toktarbaiuly [1]

[1] Renewable Energy Systems and Material Science Laboratory, National Laboratory Astana (NLA),
   Nazarbayev University, Kabanbay Batyr 53, Nur-Sultan 010000, Kazakhstan
[2] Department of Chemistry, Faculty of Natural Science, Kazakh National Woman's Teacher Training University,
   Aitekebi Street 99, Almaty 700420, Kazakhstan
[3] Department of Chemistry, Faculty of Natural Sciecnes, L.N. Gumilyov Eurasian National University,
   Kazhymukan Street 5, Nur-Sultan 010008, Kazakhstan
[4] Department of Chemistry and Chemical Technology, Faculty of Technology, Taraz Regional University
   Named after M.Kh.Dulaty, Taraz 080000, Kazakhstan
*   Correspondence: zhexenbek.toktarbay@nu.edu.kz

**Abstract:** This study has demonstrated, for the first time, the potential application of coatings to protect bricks or architectures against detrimental atmospheric effects via a self-cleaning approach. In this research, a facile fabrication method was developed to produce amorphous SiO$_2$ particles and their hierarchical structures via applying trimethylchlorosilane (TMCS). They were fully characterized by various surface analytic tools, including a goniometer, SEM, AFM, zeta sizer, and a spectroscopic technique (FTIR), and then applied as super hydrophobic coatings on glass and sand. The characterization results revealed that the SiO$_2$ particles are amorphous, quasi-spherical particles with an average diameter of 250–300 nm, and the hierarchical structures in the film were assembled from building blocks of SiO$_2$ and TMCS. The wettability of the films can be controlled by changing the pH of the SiO$_2$/TCMS dispersion. A super hydrophobic surface with a water contact angle of $165° \pm 1°$ was achieved at the isoelectric point of the films. The obtained translucent super hydrophobic SiO$_2$/TMCS coatings show good self-cleaning performances for glass and sand as construction materials. This study indicated that the superhydrophobic coatings may have potential applications in the protection of buildings and construction architectures in the future.

**Keywords:** superhydrophobic surfaces; SiO$_2$/TMCS coatings; self-cleaning; construction materials

## 1. Introduction

In recent times, pollutants from climate and environmental change are causing serious damage to the outdoor surfaces of buildings. These contaminants not only bring damage to the surface, but also remain on the surface of the building [1–5]. If these surfaces are not cleaned over time, they will depreciate the wear resistance of the building and affect the quality of the surface. Cleaning the exterior of a building is not only expensive, but also a very perilous practice. Developing multifunctional super hydrophobic materials is attractive to many researchers, since they hold surface self-cleaning and protection properties, and reduce costs. It is well known that superhydrophobic materials have excellent self-cleaning properties [6–12], and their practical applications include their use as waterproof, anti-fouling, anti-corrosion [13] and anti-rust materials [14,15]. Among them, corrosion resistance is one of the unique properties of superhydrophobic materials [16,17]. Furthermore, water contact angle (WCA) and roll-off angle (SA) are the two main important parameters used to characterize their superhydrophobic property [18]. A superhydrophobic surface possesses low surface energy and comprises a hierarchical rough structure [19].

As both WCA and SA are greater than 150° and less than 10°, respectively, they become ideal candidates for the self-cleaning application. Therefore, both a high static WCA and a low SA are major requirements for self-cleaning materials [18,20–22]. On the self-cleaning superhydrophobic surface, water droplets can easily roll and simultaneously carry away dust/dirt attached to the surface. Moreover, superhydrophobic materials have been developed from various materials, such as carbon nano-structures [22–24], silica-based nano-composites [25–28], fluorinated silanes [29–31], siloxane polymers [32–34] and two-dimensional (2D) transition metal dichalcogenides [35]. Significant efforts have been made in developing self-cleaning superhydrophobic surfaces [19].

However, protection of concrete is still a challenging task in the structural engineering field, since the desired coating is not only substrate-dependent, but also the cost has to be taken into consideration. The synthesis process of some organic particles is complex, time-consuming, harsh and costly, and can only be prepared in the laboratory [36]. In addition, to produce the self-cleaning hydrophobic coating, some superhydrophobic coatings need further baking and heating treatment after coating on the substrate surface [37,38].

Thus, the development of silica-based coatings is interesting to study since they are cost effective, easy processable materials and they have unique properties, such as excellent chemical inertness, high thermal resistance, strong mechanical strength, and tunable optical properties.

In this study, for the first time, we reported a facile fabrication method of a silica-based superhydrophobic coating system on glass and sand substrates using trimethylcholorsilane-modified $SiO_2$ nanoparticles and tested self-cleaning construction materials. The experimental results showed that the as-prepared superhydrophobic $SiO_2$/trimethylchlorosilane (TMCS) coating had a contact angle up to 165°, with a roll-off angle of less than 10° and demonstrated self-cleaning properties.

## 2. Materials and Methods

### 2.1. Materials

Tetraethoxysilane (TEOS, 98%), ethanol (96% purity), trimethylchlorosilane (TMCS, 99%), ammonium hydroxide solution (28% $NH_3$ in $H_2O$, 99.99%), and DI water were used in all the experiments. All the chemicals were purchased from Sigma Aldrich (St. Louis, MO, USA) and were used without further purification.

### 2.2. Synthesis of $SiO_2$ Nanoparticles

As in a typical synthesis process, 30 mL of ethanol was mixed with 10 mL of DI water. Later on, 2 mL of TEOS was added drop-wise. The obtained solution was heated at 30 °C and vigorously stirred (700 rpm) for 5 min. Then, a different amount of 0.5 M $NH_4OH$ (depending on the pH level) was added and left to react for 1 h to form white turbid silica solution. A schematic illustration of the process is shown in Figure 1.
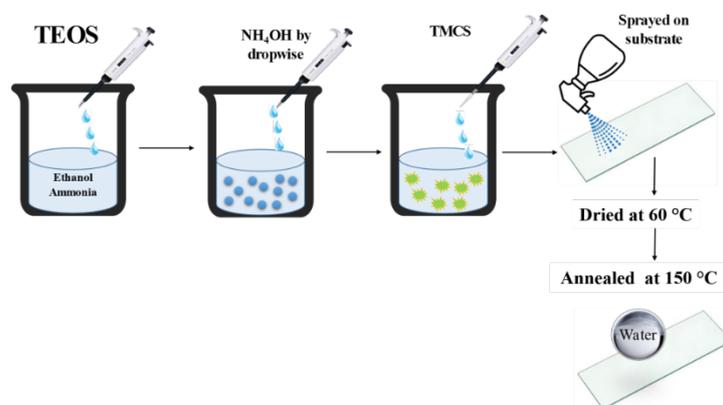


**Figure 1.** Preparation of superhydrophobic $SiO_2$/TMCS coatings onto glass.

### 2.3. Preparation of Superhydrophobic Surfaces

An amount of 25 mL of as-prepared silica solution and 5 mL of TMCS in a volume ratio of 5:1 were stirred at 700 rpm for 5 h to form the colloidal dispersion. The initial pH of the dispersion was 2.8 and different pH levels were achieved using 0.5 M $NH_4OH$. The dispersion with a pH range from 2 to 12 was used for the coating and the contact angles were measured for each pH level after spraying. The hydrophobic colloidal dispersion was sprayed onto substrates with a household sprayer. After coating, the substrates were dried under ambient conditions for 1 h, and then heated at 150 °C for 1h with an increase of 1 °C/min in order to remove the residual solvent.

### 2.4. Characterization

A zeta sizer (Malvern Zetasizer Nano ZS, Worcestershire, UK) was applied to measure the zeta ($\zeta$) potential of the colloidal particles. The formation of silica particles and their modification were investigated in powder form using an FT-IR spectrometer (ANicolet iS10, Thermo Scientific, Waltham, MA, USA). Contact angles (OCA) of water droplets on the glass and sand were measured by a goniometer (Dataphysics OCA 15Pro, Filderstadt, Germany). Scanning electron microscopy (SEM) (Zeiss Auriga Crossbeam 540, Carl Zeiss, Oberkochen, Germany) and X-ray diffraction (XRD, SmartLab, Rigaku, Tokyo, Japan) were utilized to investigate the morphology and crystal structure of nano-$SiO_2$ and functionalized $SiO_2$/TMCS.

## 3. Results and Discussion

In this study, to develop a superhydrophobic self-cleaning coating for the exterior of buildings or construction, silica-based particle systems were proposed based on the following advantages: (1) abundance on earth; (2) cost-effectiveness; (3) easily processed; and (4) similar nature to buildings. For this purpose, hydrophobic-silica particle coatings were developed to test their self-cleaning performance on glass and sand.

### 3.1. Fabrication of Superhydrophobic SiO₂/TMCS Coating

Pure $SiO_2$ NPs were synthesized by hydrolysis of TEOS in the presence of ammonia aqua solution using the Stober method [34], and then TMCS was introduced onto the surface of silica particles. Superhydrophobic properties were achieved by substitution of hydroxyl groups on the surface of the $SiO_2$ NPs with methyl groups from TMCS (Figure 2).
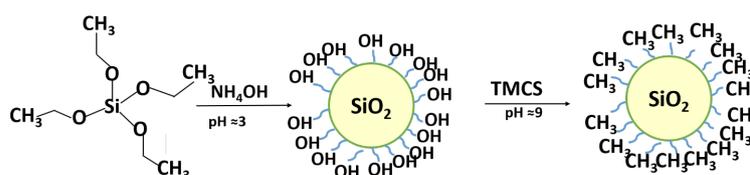


**Figure 2.** Process of formation of superhydrophobic $SiO_2$/TMCS coating.

The zeta potential, which depends on the surface charge, is important for the stability of nanoparticles in suspension. When the pH decreases, the particles tend to form agglomerates due to the absence of electrostatic stabilization of the nanoparticles that keeps them apart. As a result, silica nanoparticles functionalized with TMCS dispersion showed some precipitates. When the pH is at about 9, it reaches the isoelectrical point, where the negative and positive charges are equal on the surface of the silica particles. As the pH value increases from 9, the Z potential becomes more and more positive, indicating the increase in positive charge on the particle surface. As a result, the repulsion forces overcome the attractive forces between the nanoparticles and result in electrostatic stabilization [39]. In addition, the isoelectric point (IEP) of the as-synthesized bare silica NPs was found at pH = 2–3 (Figure 3a). This might be a feature of the condensation reaction of the silicic acids ($Si(OH)_4$). As the pH increases from 3, the negative charges increase, the repulsion forces between nanoparticles also increase and suspension tends to stabilize [40].
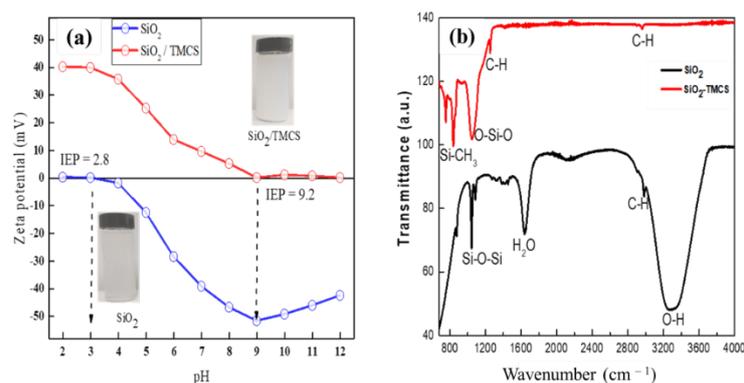
**Figure 3.** Isoelectric point (**a**) and FTIR (**b**) of SiO$_2$ NPs and SiO$_2$/TMCS film.

As shown in Figure 3b, broad absorption bands at 3400 cm$^{-1}$ and 1620 cm$^{-1}$ corresponded to the –OH groups adsorbed at the SiO$_2$ surface in the FTIR spectrum. The broad absorption bands at around 3400 cm$^{-1}$ and 1600cm$^{-1}$ corresponded to the –OH groups adsorbed at the SiO$_2$ surface, which disappeared after applying TMCS on the surface of SiO$_2$ and after annealing (Figure 3b, red line). The absorption peaks at around 1099 cm$^{-1}$ were assigned to the Si–O–Si asymmetric stretching and bending vibrations. Likewise, the characteristic peaks at 2972 cm$^{-1}$ and at 1392 cm$^{-1}$ were assigned to C–H of the CH$_3$ antisymmetric stretching vibration to the symmetric vibration and in-plane vibration of the –CH$_3$ group, respectively. It indicated the presence of CH$_3$ (hydrophobic functional group) on the surface of SiO$_2$ particles. Moreover, the peak at 765 cm$^{-1}$ that corresponded to the symmetric stretching vibration of the Si–CH$_3$ group showed the hydrophobic modification of the silica particles. The reaction between SiO$_2$ particles and TMCS was completed through the formation of the Si–O–Si bonds.

### 3.2. Investigation of Surface Morphology of SiO$_2$/TMCS Coating

The morphology of the bare SiO$_2$ NPs and the SiO$_2$ modified with TMCS coating onto glass was examined by SEM and AFM techniques. According to the SEM images (Figure 4a), bare SiO$_2$ NPs had a spherical monodisperse uniform shape and were 15–20 nm in size, and also had an amorphous structure with a wide peak at 2θ = 22.5° (Figure 4c). However, after the SiO$_2$ particles were modified by TMCS (Figure 4b,d), the surface of the materials became rough. Moreover, SiO$_2$ modified with TMCS particles formed a uniformly distributed film on the glass substrate, with sizes ranging from 100 to 300 nm and exhibited a rough surface covered by the low surface free energy of methyl groups (Si–CH$_3$) at 765cm$^{-1}$, as confirmed by FTIR (Figure 3b).
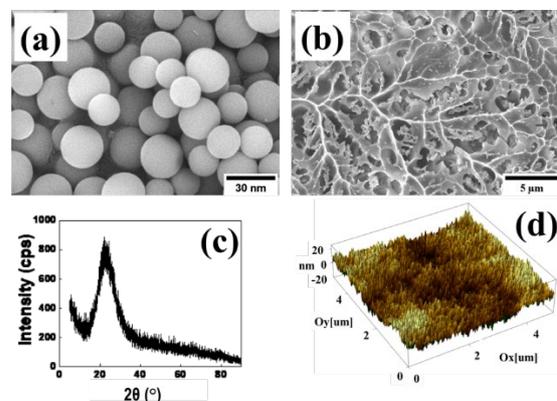


**Figure 4.** SiO$_2$ NPs (**a**) SEM and (**c**) XRD; and SiO$_2$/TMCS coatings (**b**) SEM and (**d**) AFM.

Particles of different sizes and shapes in the system resulted in the rough surface of the coatings, which is beneficial for the formation of the superhydrophobic properties. The rough surface structure is a crucial parameter to create superhydrophobic properties [41–44].

*3.3. Contact Angle (OCA) Study*

The wettability of glass and sand coated with $SiO_2$/TMCS was studied by using a goniometer (an OSA-15EC instrument). Figure 5 shows the contact angles of water droplets on the $SiO_2$ modified with TMCS superhydrophobic materials after being applied to the surface of glass and sand. Glass surfaces (Figure 5a,b) treated with $SiO_2$/TMCS slurry produced a superhydrophobic effect with a contact angle above 150°. The reason for the superhydrophobic coatings is the formation of the rough surface at IEP due to the van der Waals attraction.
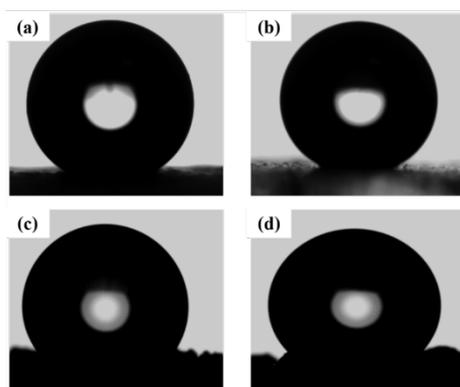


**Figure 5.** Water contact angle measurement of glass ((**a**) 159, (**b**) 165) and sand ((**c**) 150, (**d**) 148) coating with $SiO_2$/TMCS, respectively.

Figure 6 shows the effect of the pH of the $SiO_2$/TMCS dispersion on the contact angle. The wettability of coated glass was increased with the increasing pH of $SiO_2$, reaching a superhydrophobic state with a contact angle of 152° at pH = 7, 159° at pH = 8, and 165° at pH = 9. This increase in contact angle can be explained by an increase in surface roughness, due to the formation of a network of silica particles via Vander Waals attraction at the IEP point. However, after pH = 9, the contact angle sharply decreased, reaching 129°. The diagram shows that, despite the influence of the pH of $SiO_2$/TMCS dispersion, all samples showed a hydrophobic state.
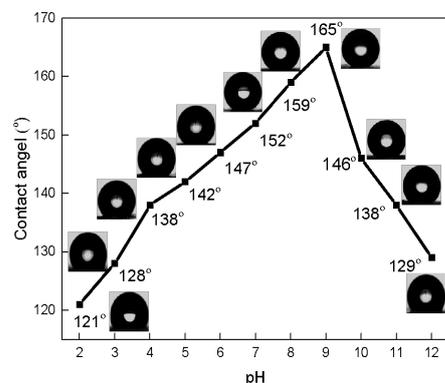


**Figure 6.** Dependence of contact angle on pH of $SiO_2$/TMCS.

The high contact angle of hydrophobized sand (151°) and glass (165°) confirmed the formation of superhydrophobic coatings (Figure 7). To evaluate the anti-icing properties of the $SiO_2$/TMCS coating, surface-coated brick and concrete were placed in a freezer at −30°C, then water was dropped over them. The water contact angle was 135°. An image of the experiment is given in the Supporting Information (Figures S1 and S2). It

can be observed from the image that the $SiO_2$/TMCS coating can be applied in extreme cold temperatures for the purpose of coating building materials. Fluidity testing of the $SiO_2$/TMCS coating on the brick can also be observed in the video in the supporting information. It can be observed that hydrophobic surfaces do not easily become wet in contact with water. The phenomenon is due to unbalanced molecular forces at the water/solids interface, which causes surface tension. Low surface energy resists wetting [45,46].
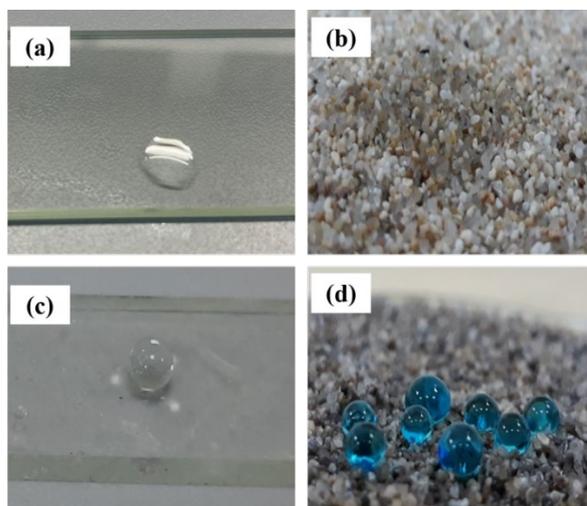


**Figure 7.** Optical images of the wetting states of water droplets on the glass before (**a**) and after treatment (**c**) and sand before (**b**) and after treatment (**d**).

*3.4. Self-Cleaning Study of Construction Materials*

Self-cleaning is a crucial property of superhydrophobic materials for practical applications. A series of experiments were conducted to demonstrate the self-cleaning properties of the coated glass. The experiments were executed following two methods, as shown in Figure 8. In the first experiment, blue color water droplets (contaminated water) were rolled from glass substrates, and the result showed no remains of tailings (Figure 8a,b). In the second experiment, dust from the sands was applied as dirt onto a superhydrophobic glass substrate for visualization of the self-cleaning process. Then, the process was observed to determine the capability of water droplets to remove the dust particles (Figure 8c,d).
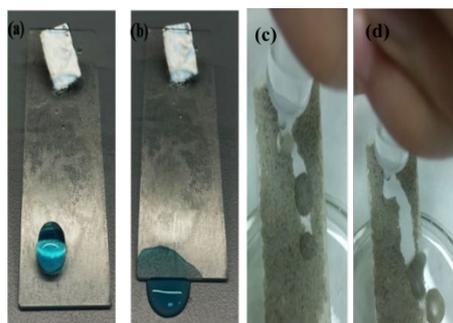


**Figure 8.** Optical images of the sliding water droplets (**a**,**b**) on the superhydrophobic surface and self-cleaning behavior of the superhydrophobic glass surfaces (**c**,**d**).

These results indicate that the coated glass substrates have good self-cleaning capabilities because the dyed water and dust did not remain on the coated glass slide after the removal of dirt by rolling water droplets. $SiO_2$ modified with TMCS coatings possesses superhydrophobic properties due to the surface roughness by creating the hierarchical rough structure and low surface free energy of methyl groups. These properties could maintain the water droplets in the 'solid–vapor–liquid phase' through forming a high-water contact angle ($90° < \theta < 150°$) and a low-water roll-off angle ($10°$). Consequently,

the two mentioned characteristics of the as-prepared superhydrophobic glass caused the water droplets to easily roll off over the modified surface without moistening the surface, meaning that contaminants will be easier to remove.

## 4. Conclusions

Bare $SiO_2$ nanoparticles and $SiO_2$ modified with TMCS nanocomposites were successfully synthesized, characterized and used as self-cleaning coatings. The results showed that nano-sized $SiO_2$ particles had spherical, monodisperse and uniform shapes. XRD analysis of $SiO_2$ indicates a wide peak located approximately at $2\theta = 22.5°$, which suggests an amorphous structure. The SEM results indicate that, after $SiO_2$ particles were modified with TMCS, the surface of the coatings became rough. It was found that the coatings demonstrated excellent superhydrophobic and self-cleaning properties. The highest contact angle was recorded as $165°$ at pH = 9. The proposed coatings may have potential applications in the protection of buildings and constructions.

**Supplementary Materials:** The following supporting information can be downloaded at: https://www.mdpi.com/article/10.3390/coatings12101422/s1, Figure S1: Optical images of the wetting states of water droplets on the brick at 30 °C; Figure S2: Optical images of the wetting states of water droplets on the concrete at 30 °C; Figure S3: Fluidity test on the concrete; Figure S4: Self-cleaning test on the concrete.

**Author Contributions:** Data curation, R.K., A.T. and A.K.; Investigation, A.K., T.Z., A.S., N.A., Y.K. and O.T.; Methodology, A.S., Z.T., N.M., K.K. and O.T.; Project administration, O.T.; Resources, R.K.; Writing—original draft, A.K. and M.N.; Writing—review and editing, Z.T. and O.T. All authors have read and agreed to the published version of the manuscript.

**Institutional Review Board Statement:** Not applicable.

**Informed Consent Statement:** Not applicable.

**Data Availability Statement:** Not applicable.

**Conflicts of Interest:** The authors declare no conflict of interest.

## References

1. Belfiore, C.M.; Barca, D.; Bonazza, A.; Comite, V.; La Russa, M.F.; Pezzino, A.; Ruffolo, S.A.; Sabbioni, C. Application of spectrometric analysis to the identification of pollution sources causing cultural heritage damage. *Environ. Sci. Pollut. Res.* **2013**, *20*, 8848–8859. [CrossRef]
2. Akhmetzhan, A.; Myrzakhmetova, N.; Amangeldi, N.; Kuanyshova, Z.; Akimbayeva, N.; Dosmaganbetova, S.; Toktarbay, Z.; Longinos, S.N. A Short Review on the N,N-Dimethylacrylamide-Based Hydrogels. *Gels* **2021**, *7*, 234. [CrossRef]
3. Kronlund, D.; Bergbreiter, A.; Lindén, M.; Grosso, D.; Smått, J.-H. Hydrophobization of marble pore surfaces using a total immersion treatment method—Influence of co-solvents and temperature on fluorosurfactant vesicle behavior. *Colloids Surf. A Physicochem. Eng. Asp.* **2015**, *483*, 104–111. [CrossRef]
4. Abdiyev, K.Z.; Maric, M.; Orynbayev, B.Y.; Toktarbay, Z.; Zhursumbaeva, M.B.; Seitkaliyeva, N.Z. Flocculating properties of 2-acrylamido-2-methyl-1-propane sulfonic acid-co-allylamine polyampholytic copolymers. *Polym. Bull.* **2022**, 1–16. [CrossRef]
5. Xue, C.-H.; Jia, S.-T.; Zhang, J.; Ma, J.-Z. Large-area fabrication of superhydrophobic surfaces for practical applications: An overview. *Sci. Technol. Adv. Mater.* **2010**, *11*, 033002. [CrossRef]
6. Liu, Y.; Liu, J.; Li, S.; Wang, Y.; Han, Z.; Ren, L. One-step method for fabrication of biomimetic superhydrophobic surface on aluminum alloy. *Colloids Surf. A Physicochem. Eng. Asp.* **2015**, *466*, 125–131. [CrossRef]
7. Nuraje, N.; Asmatulu, R.; Cohen, R.E.; Rubner, M.F. Durable Antifog Films from Layer-by-Layer Molecularly Blended Hydrophilic Polysaccharides. *Langmuir* **2011**, *27*, 782–791. [CrossRef]
8. Erbil, H.Y. Practical Applications of Superhydrophobic Materials and Coatings: Problems and Perspectives. *Langmuir* **2020**, *36*, 2493–2509. [CrossRef]
9. Zhao, S.; Liang, Y.; Yang, Y.; Huang, J.; Guo, Z.; Liu, W. A robust surface with superhydrophobicity and underwater superoleophobicity for on-demand oil/water separation. *Nanoscale* **2021**, *13*, 15334–15342. [CrossRef]

10. Kudaibergenova, R.; Ualibek, O.; Sugurbekov, E.; Demeuova, G.; Frochot, C.; Acherar, S.; Sugurbekova, G. Reduced graphene oxide-based superhydrophobic magnetic nanomaterial as high selective and recyclable sorbent for oil/organic solvent wastewater treatment. *Int. J. Environ. Sci. Technol.* **2022**, *19*, 8491–8506. [CrossRef]

11. Nuraje, N.; Khan, W.; Ceylan, M.; Lei, Y.; Asmatulu, R. Superhydrophobic electrospun nanofibers. *J. Mater. Chem. A* **2013**, *1*, 1929. [CrossRef]

12. Asmatulu, R.; Ceylan, M.; Nuraje, N. Study of superhydrophobic electrospun nanocomposite fibers for energy systems. *Langmuir* **2011**, *27*, 504–507. [CrossRef]

13. Jishnu, A.; Jayan, J.S.; Saritha, A.; Sethulekshmi, A.S.; Venu, G. Superhydrophobic graphene-based materials with self-cleaning and anticorrosion performance: An appraisal of neoteric advancement and future perspectives. *Colloids Surf. A Physicochem. Eng. Asp.* **2020**, *606*, 125395. [CrossRef]

14. Zhao, X.; Abutalip, M.; Afroz, K.; Nuraje, N. Hydrophobically modified polycarboxybetaine: From living radical polymerization to self-assembly. *Langmuir* **2018**, *35*, 1606–1612. [CrossRef]

15. Wang, Z.; Paul, S.; Stein, L.H.; Salemi, A.; Mitra, S. Recent Developments in Blood-Compatible Superhydrophobic Surfaces. *Polymers* **2022**, *14*, 1075. [CrossRef]

16. Zhang, Z.-Q.; Wang, L.; Zeng, M.-Q.; Zeng, R.-C.; Lin, C.-G.; Wang, Z.-L.; Chen, D.-C.; Zhang, Q. Corrosion resistance and superhydrophobicity of one-step polypropylene coating on anodized AZ31 Mg alloy. *J. Magnes. Alloys* **2021**, *9*, 1443–1457. [CrossRef]

17. Wang, Z.; Yang, W.; Sun, F.; Zhang, P.; He, Y.; Wang, X.; Luo, D.; Ma, W.; Sergio, G.-C. Construction of a superhydrophobic coating using triethoxyvinylsilane-modified silica nanoparticles. *Surf. Eng.* **2019**, *35*, 418–425. [CrossRef]

18. Liu, H. Robust translucent superhydrophobic PDMS/PMMA film by facile one-step spray for self-cleaning and efficient emulsion separation. *Chem. Eng. J.* **2017**, *330*, 26–35. [CrossRef]

19. Xiang, T.; Lv, Z.; Wei, F.; Liu, J.; Dong, W.; Li, C.; Zhao, Y.; Chen, D. Superhydrophobic Civil Engineering Materials: A Review from Recent Developments. *Coatings* **2019**, *9*, 753. [CrossRef]

20. Yang, C.; Hao, P.; He, F. Effect of upper contact line on sliding behavior of water droplet on superhydrophobic surface. *Sci. Bull.* **2009**, *54*, 727–731. [CrossRef]

21. Yi, M.; Liu, L.; Wu, L.; Li, X. Research on sliding angles of water droplets on the hierarchical structured superhydrophobic surfaces. *Appl. Phys. A* **2020**, *126*, 47. [CrossRef]

22. Xiang, S.; Liu, W. Self-Healing Superhydrophobic Surfaces: Healing Principles and Applications. *Adv. Mater. Interfaces* **2021**, *8*, 2100247. [CrossRef]

23. Longinos, S.K.; Longinou, D.-D.; Celebi, E.; Toktarbay, Z.; Parlaktuna, M. Kinetic study of methane hydrate formation with the use of a surface baffle. *React. Kinet. Mech. Catal.* **2021**, *134*, 75–86. [CrossRef]

24. Abdelmagid, G.; Yilbas, B.S.; Al-Sharafi, A.; Al-Qahtani, H.; Al-Aqeeli, N. Water droplet on inclined dusty hydrophobic surface: Influence of droplet volume on environmental dust particles removal. *RSC Adv.* **2019**, *9*, 3582–3596. [CrossRef]

25. Sun, C.; Lyu, Q.; Si, Y.; Tong, T.; Lin, L.-C.; Yang, F.; Tang, C.Y.; Dong, Y. Superhydrophobic Carbon Nanotube Network Membranes for Membrane Distillation: High-Throughput Performance and Transport Mechanism. *Environ. Sci. Technol.* **2022**, *56*, 5775–5785. [CrossRef]

26. Chen, X.; Yang, M.; Zhao, X.; Hu, D.; Liu, W.; Ma, W. Tailoring superhydrophobic PDMS/CeFe$_2$O$_4$/MWCNTs nanocomposites with conductive network for highly efficient microwave absorption. *Chem. Eng. J.* **2022**, *432*, 134226. [CrossRef]

27. Zulkharnay, R.; Ualibek, O.; Toktarbaiuly, O.; May, P.W. Hydrophobic behaviour of reduced graphene oxide thin film fabricated via electrostatic spray deposition. *Bull. Mater. Sci.* **2021**, *44*, 112. [CrossRef]

28. Ibrahim, S.; Sultan, M. Superhydrophobic Coating Polymer/Silica Nanocomposites: Part I Synthesis and Characterization as Eco-Friendly Coating. *Silicon* **2020**, *12*, 805–811. [CrossRef]

29. Wang, X.; Li, X.; Lei, Q.; Wu, Y.; Li, W. Fabrication of superhydrophobic composite coating based on fluorosilicone resin and silica nanoparticles. *R. Soc. Open Sci.* **2018**, *5*, 180598. [CrossRef]

30. Kim, G.-H.; Kang, D.-H.; Jung, B.-N.; Shim, J.-K. Fabrication and Characterization of Hydrophobic Cellulose Nanofibrils/Silica Nanocomposites with Hexadecyltrimethoxysilane. *Polymers* **2022**, *14*, 833. [CrossRef]

31. Xu, B.; Zhang, Q. Preparation and Properties of Hydrophobically Modified Nano-SiO$_2$ with Hexadecyltrimethoxysilane. *ACS Omega* **2021**, *6*, 9764–9770. [CrossRef]

32. Cai, Y.; Li, J.; Yi, L.; Yan, X.; Li, J. Fabricating superhydrophobic and oleophobic surface with silica nanoparticles modified by silanes and environment-friendly fluorinated chemicals. *Appl. Surf. Sci.* **2018**, *450*, 102–111. [CrossRef]

33. Jeong, H.; Baek, S.; Han, S.; Jang, H.; Rockson, T.K.; Lee, H.S. Chemically Robust Superhydrophobic Poly(vinylidene fluoride) Films with Grafting Crosslinkable Fluorinated Silane. *Macromol. Res.* **2018**, *26*, 493–499. [CrossRef]

34. Stöber, W.; Fink, A.; Bohn, E. Controlled growth of monodisperse silica spheres in the micron size range. *J. Colloid Interface Sci.* **1968**, *26*, 62–69. [CrossRef]

35. Kim, H.; Nam, K.; Lee, D.Y. Fabrication of Robust Superhydrophobic Surfaces with Dual-Curing Siloxane Resin and Controlled Dispersion of Nanoparticles. *Polymers* **2020**, *12*, 1420. [CrossRef] [PubMed]

36. Hou, B.; Li, X.; Ma, X.; Du, C.; Zhang, D.; Zheng, M.; Xu, W.; Lu, D.; Ma, F. The cost of corrosion in China. *npj Mater. Degrad.* **2017**, *1*, 4. [CrossRef]

37. Ma, J.; Zhang, X.; Bao, Y.; Liu, J. A facile spraying method for fabricating superhydrophobic leather coating. *Colloids Surf. A Physicochem. Eng. Asp.* **2015**, *472*, 21–25. [CrossRef]

38. Ogihara, H.; Xie, J.; Okagaki, J.; Saji, T. Simple Method for Preparing Superhydrophobic Paper: Spray-Deposited Hydrophobic Silica Nanoparticle Coatings Exhibit High Water-Repellency and Transparency. *Langmuir* **2012**, *28*, 4605–4608. [CrossRef]

39. Sikora, A.; Shard, A.G.; Minelli, C. Size and $\zeta$-Potential Measurement of Silica Nanoparticles in Serum Using Tunable Resistive Pulse Sensing. *Langmuir* **2016**, *32*, 2216–2224. [CrossRef]

40. Xu, P.; Wang, H.; Tong, R.; Du, Q.; Zhong, W. Preparation and morphology of $SiO_2$/PMMA nanohybrids by microemulsion polymerization. *Colloid Polym. Sci.* **2006**, *284*, 755–762. [CrossRef]

41. Boinovich, L.; Emelyanenko, A. Principles of Design of Superhydrophobic Coatings by Deposition from Dispersions. *Langmuir* **2009**, *25*, 2907–2912. [CrossRef]

42. Ding, K.; Wang, C.; Li, S.; Zhang, X.; Lin, N. Large-area cactus-like micro-/nanostructures with anti-reflection and superhydrophobicity fabricated by femtosecond laser and thermal treatment. *Surf. Interfaces* **2022**, *33*, 102292. [CrossRef]

43. Wang, P.; Li, C.; Zhang, D. Recent advances in chemical durability and mechanical stability of superhydrophobic materials: Multi-strategy design and strengthening. *J. Mater. Sci. Technol.* **2022**, *129*, 40–69. [CrossRef]

44. Song, Y.; Wang, C.; Dong, X.; Yin, K.; Zhang, F.; Xie, Z.; Chu, D.; Duan, J. Controllable superhydrophobic aluminum surfaces with tunable adhesion fabricated by femtosecond laser. *Opt. Laser Technol.* **2018**, *102*, 25–31. [CrossRef]

45. Yessimova, O.; Kumargaliyeva, S.; Kerimkulova, M.; Mussabekov, K.; Toktarbay, Z. Wetting ability of a phytopreparation and their associates with polyelectrolytes. *Rasayan J. Chem.* **2020**, *13*, 481–487. [CrossRef]

46. Toktarbaiuly, O.; Syrlybekov, A.; Mauit, O.; Kurbanova, A.; Sugurbekova, G.; Shvets, I. Magnetic and electronic properties of $Fe_3O_4$/$PtSe_2$/$Fe_3O_4$ junctions. *Mater. Today Proc.* **2022**, *49*, 2469–2473. [CrossRef]